AD-A094 354 MARYLAND UNIV COLLEGE PARK COMPUTER VISION LAB F/G 9/2
SPATIAL AUTOREGRESSIONS IN DIGITAL IMAGE RESTORATION: SIMULTANE--ETC(U)
DEC 80 R CHELLAPPA AFOSR-77-3271
UNCLASSIFIED TR-984 AFOSR-TR-81-0059 NL

1 of 1

END
DATE
FILMED
2-81
DTIC

AFOSR-TR- 81-0059

LEVEL

AD A094354

COMPUTER SCIENCE
TECHNICAL REPORT SERIES

SELECTED
FEB 2 1981
A

UNIVERSITY OF MARYLAND
COLLEGE PARK, MARYLAND
20742

DDC FILE COPY

81 2 2 074

UNCLASSIFIED

SECURITY CLASSIFICATION OF THIS PAGE (When Data Entered)

REPORT DOCUMENTATION PAGE

READ INSTRUCTIONS BEFORE COMPLETING FORM

19

1. REPORT NUMBER: 18 AFOSR-TR-81-0059	2. GOVT ACCESSION NO.: AD-A094354
3. RECIPIENT'S CATALOG NUMBER: 9	
4. TITLE (and Subtitle): 6 SPATIAL AUTOREGRESSIONS IN DIGITAL IMAGE RESTORATION: SIMULTANEOUS MODELS.	5. TYPE OF REPORT & PERIOD COVERED: INTERIM rept.
	6. PERFORMING ORG. REPORT NUMBER
7. AUTHOR(s): 10 R. Chellappa 14 TR-984	8. CONTRACT OR GRANT NUMBER(s): 15 AFOSR-77-3271
9. PERFORMING ORGANIZATION NAME AND ADDRESS: Computer Vision Laboratory, Computer Science Center, University of Maryland, College Park, MD 20742	10. PROGRAM ELEMENT, PROJECT, TASK AREA & WORK UNIT NUMBERS: 61102F 2304/A2
11. CONTROLLING OFFICE NAME AND ADDRESS: Math. & Info. Sciences, AFOSR/NM Bolling AFB Washington, DC 20332	12. REPORT DATE: 11 Dec[redacted]980
	13. NUMBER OF PAGES: 23
14. MONITORING AGENCY NAME & ADDRESS (if different from Controlling Office): 16 2304 12 26	15. SECURITY CLASS. (of this report): Unclassified 17 A2
	15a. DECLASSIFICATION/DOWNGRADING SCHEDULE

16. DISTRIBUTION STATEMENT (of this Report)

Approved for public release; distribution unlimited.

17. DISTRIBUTION STATEMENT (of the abstract entered in Block 20, if different from Report)

18. SUPPLEMENTARY NOTES

19. KEY WORDS (Continue on reverse side if necessary and identify by block number)

Image restoration
Image processing
Image models
Random fields
Autoregressive models

20. ABSTRACT (Continue on reverse side if necessary and identify by block number)

We consider the application of spatial autoregressive random field models in the restoration of degraded images. The degradation is assumed to be due to a space invariant, periodic, non-separable point spread function and additive noise, colored or white. We assume that the images are represented by two-dimensional spatial autoregressive models and we develop fast, optimal, non-recursive filters, the optimality criterion being the minimum

mean squared error (MMSE). Within the class of spatial autoregressive models, there are two nonequivalent classes of random field (RF) models, the so-called simultaneous autoregressive (SAR) models and the conditional Markov (CM) models. In this paper, we develop restoration algorithms and give examples of restoration using the SAR models. The restoration filter is optimal, if the parameters characterizing the RF models are known exactly. In practice, however, they are estimated from the images. An iterative scheme is used for the estimation of parameters in SAR models. Performance bounds of restoration algorithms are calculated. In a subsequent paper, the case of CM models will be considered.

TR-984 December, 1980
AFOSR-77-3271

SPATIAL AUTOREGRESSIONS IN DIGITAL IMAGE RESTORATION: SIMULTANEOUS MODELS

R. Chellappa
Computer Vision Laboratory
Computer Science Center
University of Maryland
College Park, MD 20742

A

ABSTRACT

We consider the application of spatial autoregressive random field models in the restoration of degraded images. The degradation is assumed to be due to a space invariant, periodic, non-separable point spread function and additive noise, colored or white. We assume that the images are represented by two-dimensional spatial autoregressive models and we develop fast, optimal, non-recursive filters, the optimality criterion being the minimum mean squared error (MMSE). Within the class of spatial autoregressive models, there are two nonequivalent classes of random field (RF) models, the so-called simultaneous autoregressive (SAR) models and the conditional Markov (CM) models. In this paper, we develop restoration algorithms and give examples of restoration using the SAR models. The restoration filter is optimal, if the parameters characterizing the RF models are known exactly. In practice, however, they are estimated from the images. An iterative scheme is used for the estimation of parameters in SAR models. Performance bounds of restoration algorithms are calculated. In a subsequent paper, the case of CM models will be considered.

The support of the U.S. Air Force Office of Scientific Research under Grant AFOSR-77-3271 is gratefully acknowledged, as is the help of Kathryn Riley in preparing this paper. The author is grateful to Prof. R. L. Kashyap and Prof. A. Rosenfeld for helpful discussions.

1. Introduction

The restoration of degraded images has many fields of application, including space imagery and biomedical images [1-2]. Several approaches have been suggested in the literature using recursive Kalman filter type algorithms [3-5], inverse filtering methods, and two-dimensional discrete partial difference equations [6-7]. The Kalman filter algorithms insist on the assumption of an underlying causal representation for the images displayed as a state space model. The various Kalman filter methods differ from one another basically regarding the assumptions that they make about the autocorrelation function. Much attention has been paid to exponential separable correlation functions in the literature. Also, the optimality with respect to MMSE claimed in Kalman filter type algorithms is valid only when the parameters of the underlying RF models are exactly known. In practice, the parameters of the model are estimated from the images, and substituted for the unknown parameters. Optimality, with respect to some criterion, can be claimed only if estimation of the parameters and minimization of the mean square error are tackled simultaneously so as to minimize the criterion function. Detailed discussions on inverse filtering approaches may be found in [1-2].

Recently [6-7], stochastic representations of digital images by finite difference approximations of partial differential equations (PDE) have been used to develop restoration algorithms. Corresponding to the PDE classification of hyperbolic, parabolic,

and elliptic systems, three different algorithms, viz., the causal, semicausal and noncausal algorithms, have been developed. By making appropriate assumptions regarding the boundary pixels, the original observations are decomposed into two parts such that the covariance matrix corresponding to one set is diagonalized by sine transforms and the other part corresponds to the boundary response. The important feature is that the eigenfunction expansion of the covariance matrix in terms of sine functions enables fast implementation of the restoration filters.

We consider the use of spatial autoregressive models for the image restoration problem. Within the family of spatial autoregressive models, there are two nonequivalent classes of RF models, the so-called simultaneous autoregressive (SAR) [8-10] models and the conditional Markov (CM) [10-13] models. These models characterize the statistical dependency of a pixel on its neighbors by a linear weighted sum of neighboring pixels and additive noise, independent or correlated depending upon whether the models are simultaneous or conditional. The structure of these models can be explained as follows: suppose we are given an observation set $\{y(s),\ s = (i,j)\in\Omega\}$, $\Omega=\{s = (i,j)\ 1\leq i,j\leq M\}$, where $y(s)$ is the observation at location s. Then the expectation of $y(s)$, conditional on all $y(s_1)$, $s_1\in\Omega, s_1\neq s$, is only a function of the observations at positions belonging to the neighbor set for the conditional models, whereas for the simultaneous models, the conditional expectation is a function of observations at positions belonging

to the neighbor set and some extra neighbors. For instance, the conditional expectation of a four neighbor simultaneous model with dependence on east, west, north and south neighbors is a function of eight nearest neighbors and second nearest neighbors on the east, west, north and south. These two classes of models are non-equivalent, in that given a SAR model, an equivalent CM model can always be found (usually with more parameters); however, the converse is not true. For instance, there is no equivalent SAR model for the CM model with dependence on the east, west, north and south neighbors. In this paper, we are primarily concerned with the use of SAR models for the digital image restoration problem. Similar results for CM models will be given later. For some results concerning the use of conditional models in image restoration, the reader is referred to [5,14].

For a finite image, the neighbors in all directions are not defined for boundary pixels. Some assumptions have to be made regrading the distribution of boundary pixels. In this report, we assume that the given finite images are represented on a torus lattice. This representation on torus lattices leads to covariance matrices that have block circulant structures. Since block circulant matrices are diagonalized by Fourier vectors, FFT computations can be used for the implementation of restoration filters. Circulant approximations to Toeplitz covariance structures have been considered in the image restoration literature. But the

block circulant structure that arises in our case is due to the underlying RF model. Consequently, the covariance matrices are exactly block circulant.

Using the specific representation mentioned above for the images, the restoration problem is then posed as one of minimizing the mean square error between the original and the restored image. This assumes that the SAR model is completely specified, i.e., the parameters characterizing the SAR model are known. In practice, however, these parameters are unknown and are estimated from the images. For SAR models that include dependency in all directions, the Jacobian of the transformation matrix from the noisy variates to the observations is not unity, leading to a log likelihood function that is nonquadratic in the parameters. Direct minimization of the log likelihood function using "off the shelf" computer programs might lead to a slow convergence rate. Consequently, an iterative scheme suggested elsewhere [15-16] is used for estimating the parameters.

The organization of the paper is as follows: In Section 2, we pose the restoration problem using the SAR models and derive its optimal filter, given the parameters of the SAR model. A brief discussion is given regarding the estimation of unknown parameters in SAR models. Performance bounds for the restoration algorithms are also derived. Several examples of restorations are given in Section 3. Finally, discussion is given in Section 4.

2. Restoration Schemes Using the Simulataneous Random Field Models

2.1 Derivation of the Optimal Filter

Consider an MxM zero mean, undegraded image represented by a two-dimensional array of gray levels, $\{y(s), s=(i,j)\ \Omega\}, \Omega=\{s=(i,j), 1\le i,j\le M\}$ where $y(s)$ is the gray level of the cell s. Since for a finite image, some of the neighbors for the boundary points are not defined, the image is assumed to be folded into a torus so that (2.1) is satisfied:

$$y[(s)+(i_1,j_1)]=y[\{(s)+(i_1-M,j_1-M)\}(\text{mod } M+1, \text{mod } M+1)] \qquad (2.1)$$

Assume that the original image $y(s)$ obeys the SAR model

$$y(s)=\sum_{(i,j)\in N}\theta_{i,j}y(s+(i,j))+\sqrt{\rho}w(s),\ s\ \Omega \qquad (2.2)$$

In (2.2), $\{w(s), s\in\Omega\}$ is a sequence of independent and indentically distributed random variables of *zero mean and unit variance* and N denotes the neighbor set, i.e., the set of neighbors on which the observation at $y(s)$ is dependent. Equation (2.2) is characterized by a set of parameters $\{\theta_{i,j},(i,j)\in N,\rho)$. Typically, N might include the members $\{(-1,0),(0,1),(1,0),(0,-1)\}$ corresponding to nearest neighbors in north, east, south, and west directions, or N might be $N=\{(-1,0),(1,1),(0,1),(1,0),(0,-1)\}$. One of the characteristics of the model in (2.2) is that, when the parameters corresponding to symmetric neighbor sets are interchanged, the resulting model has second order properties identical to the original. Denoting $\underset{\sim}{y}$ and $\underset{\sim}{w}$ as M^2x1 vectors of lexicographically ordered arrays $\{y(\cdot)\}$ and $\{w(\cdot)\}$, (2.2) can be written as

$$B(\underset{\sim}{\theta})\underset{\sim}{y} = \sqrt{P}\underset{\sim}{w} \qquad (2.3)$$

where $B(\underset{\sim}{\theta})$ is an M^2xM^2 block circulant matrix and has the following structure:

$$
\underset{\sim}{B}(\underset{\sim}{\theta}) = \begin{bmatrix} B_{1,1} & B_{1,2} & \cdots & B_{1,M} \\ B_{1,M} & B_{1,1} & \cdots & B_{1,M-1} \\ B_{1,M-1} & \cdots & B_{1,1} & B_{1,M-2} \\ \cdots & \cdots & \cdots & \cdots \\ B_{1,2} & \cdots & \cdots & B_{1,1} \end{bmatrix}
$$

where each of the component matrices is circulant. For the case $N=\{(0,1),(1,1),(0,-1),(-1,0)\}$,

$$B_{1,1}=\text{circulant }(1,\theta_{0,1},\ldots,\theta_{0,-1})$$

$$B_{1,2}=\text{circulant }(\theta_{1,1},0,\ldots,0)$$

$$B_{1,M}=\text{circulant }(\theta_{-1,0},0,\ldots,0)$$

and

$$B_{1,j}=0 \quad j\neq 1,2,\ldots,M.$$

Assuming that $B(\underset{\sim}{\theta})$ has an inverse, we have

$$\underset{\sim}{y} = \sqrt{\rho}\; B(\underset{\sim}{\theta})^{-1}\underset{\sim}{w} \tag{2.4}$$

and the image covariance matrix

$$\underset{\sim}{Q} = E(\underset{\sim}{y}\underset{\sim}{y}^T) = \rho[B^T(\underset{\sim}{\theta})B(\underset{\sim}{\theta})]^{-1} \tag{2.5}$$

is also block circulant.

Consider the case when the image $\underset{\sim}{y}$ is degraded by a non-separable, spatially invariant, periodic PSF represented by a block circulant matrix $\underset{\sim}{H}$ and an additive colored noise $\eta(s), s\in\Omega$. Thus if $\underset{\sim}{x}$ and $\underset{\sim}{\eta}$ denote M^2x1 vectors of lexicographic ordered arrays $\{x(\cdot)\}$ and $\{\eta(\cdot)\}$, where $\eta(\cdot)$ is zero mean, signal independent additive noise with known circular correlation structure,

$$E(\underset{\sim}{\eta}\underset{\sim}{\eta}^T) = \underset{\sim}{C} \text{ (a block circulant matrix)} \tag{2.6}$$

we have

$$\underset{\sim}{x} = \underset{\sim}{H}\underset{\sim}{Y}+\underset{\sim}{\eta} \tag{2.7}$$

We assume for the present that the PSF matrix $\underset{\sim}{H}$ and the parameters $(\underset{\sim}{\theta},\rho)$ in (2.2) as well as the matrix $\underset{\sim}{C}$ in (2.6) are completely known. We also assume that the degraded image fits completely inside their recording frame. In other words, the problems due to truncation of the degraded image by a finite *recording frame* are not considered. The restoration problem is posed as follows: determine $\underset{\sim}{\hat{x}}$, a function of $\underset{\sim}{x}$, such that the mean squared error f is a minimum where

$$f = (\underset{\sim}{y}-\underset{\sim}{\overline{x}})^T(\underset{\sim}{y}-\underset{\sim}{\overline{x}}) \tag{2.8}$$

and $\underset{\sim}{\hat{x}}$ is that minimizing value of $\underset{\sim}{\overline{x}}$. The optimal estimate $\underset{\sim}{\hat{x}}$ has the following expression [1, p. 133]:

$$\underset{\sim}{\hat{x}} = \underset{\sim}{Q}\ \underset{\sim}{H}^T(\underset{\sim}{H}\underset{\sim}{Q}\underset{\sim}{H}^T+\underset{\sim}{C})^{-1}\underset{\sim}{x} \tag{2.9}$$

Let $\underset{\sim}{f}_{ij}=\text{col}[\underset{\sim}{t}_j,\lambda_i t_j,\ldots,\lambda_i^{M-1}t_j],(i,j)=1,\ldots,M$

$\underset{\sim}{t}_j=\text{col}[1,\lambda_j,\lambda_j^2,\ldots,\lambda_j^{M-1}]$, M=vector

$\lambda_i=\exp[\sqrt{-1}\lambda_0(i-1)],\lambda_0=2\pi/M.$

Let $\overline{h}_{ij},\mu_{ij}$, and $\overline{c}_{ij},1\leq i,j\leq M$ denote the M^2 eigenvalues of the block circulant matrices, $\underset{\sim}{H}$, $B(\underset{\sim}{\theta})$ and $\underset{\sim}{C}$ respectively. Then from the theory of circulant matrices,

$$\mu_{ij}=(1-\underset{\sim}{\theta}^T\underset{\sim}{\psi}_{ij}) \tag{2.10}$$

$$\overline{h}_{ij}=(h_{00}+\underset{\sim}{h}^T\underset{\sim}{\psi}_{ij})$$

where

$$\underset{\sim}{\psi}_{ij}=\text{col}[\exp(\sqrt{-1}\ \tfrac{2\pi}{M}((i-1)k+(j-1)\ell)),\ (k,\ell)\in N]$$

and $\underset{\sim}{h}=\text{col}[h_{i,j},0\leq(i,j)\leq p,(i,j)\neq(0,0)]$

and p is the width of the PSF. Using the fact that the Fourier vectors $\underset{\sim}{f}_{ij}$ are the eigenvectors of $\underset{\sim}{Q}$, $\underset{\sim}{H}$, and $\underset{\sim}{C}$, with the corresponding eigenvalues $\rho/||\mu_{ij}||^2$, $\bar{h}_{ij}$ and $\bar{c}_{ij}$, the following expression can be written for $\hat{\underset{\sim}{x}}$:

$$\hat{\underset{\sim}{x}} = \frac{1}{M^2}\sum_{\Omega} \underset{\sim}{f}_{ij}(\rho\bar{h}^*_{ij}/(\rho||\bar{h}_{ij}||^2+\bar{c}_{ij}||\mu_{ij}||^2))\underset{\sim}{f}^{*T}_{ij}\ \underset{\sim}{x} \tag{2.11}$$

where * denotes the complex conjugate operator. The computation of $\hat{\underset{\sim}{x}}$ can be done by using FFT and the computational complexity is $O(M^2\log M)$. The following special cases of (2.1) are of interest.

<u>Case i</u> (Additive noise η is white with variance γ): For this case, $\underset{\sim}{C}=\underset{\sim}{\gamma}\ \underset{\sim}{I}$ and $\hat{\underset{\sim}{x}}$ reduces to

$$\hat{\underset{\sim}{x}} = \frac{1}{M^2}\sum_{\Omega} \underset{\sim}{f}_{ij}(\rho\bar{h}^*_{ij}/(\rho||\bar{h}_{ij}||^2+\gamma||\mu_{ij}||^2))\underset{\sim}{f}^{*T}_{ij}\ \underset{\sim}{x} \tag{2.12}$$

<u>Case ii</u> (Degradation is due to white noise only): For this case, $\underset{\sim}{H}=\underset{\sim}{I}$ and hence $\hat{\underset{\sim}{x}}$ reduces to

$$\hat{\underset{\sim}{x}} = \frac{1}{M^2}\sum_{\Omega} \underset{\sim}{f}_{ij}\ \frac{\rho}{(\rho+\gamma||\mu_{ij}||^2)}\ \underset{\sim}{f}^{*T}_{ij}\ \underset{\sim}{x} \tag{2.13}$$

The restoration algorithms given above have a general structure that is valid for the so-called causal, semicausal and non-causal neighbor sets. (Actually, due to the torus assumption, the neighbor set $N=\{(-1,0),(0,-1),(-1,-1)\}$ does not correspond to a

strictly causal model, but the error in approximation due to torus structure is very small for causal neighbor sets.) We have not made any special assumptions such as isotropy, etc.

Thus far we have assumed that the parameters $\underset{\sim}{\theta}, \rho$ characterizing the original image are known. In practice, however, they are estimated from the original image and the estimated parameters are used in place of true parameters in the restoration algorithms.

2.2 Parameter Estimation

The popular methods of estimation are the method of least squares (LS) and of maximum likelihood (ML). However, the classical LS estimates are not in general consistent, when we consider SAR models that include neighbor set dependence in all the directions [8]. The ML estimation scheme involves obtaining an expression for the likelihood of the observations. We first assume that $\{w(\cdot)\}$ is distributed normally with zero mean and unit variance. To ensure stationarity, assume $|\mu_{ij}(\underset{\sim}{\theta})| \neq 0$, $i,j=1,\ldots,M$. By using the property of the noise $\{w(\cdot)\}$ and (2.1), the log likelihood of observations $\ell n p(\underset{\sim}{y}|\underset{\sim}{\theta},\rho)$ can be written as

$$\ell n\, p(\underset{\sim}{y}|\underset{\sim}{\theta},\rho) = \ell n \det B(\underset{\sim}{\theta}) - (M^2/2)\ell n 2\pi\rho - \frac{1}{2\rho}\sum_{\Omega}(y(s)-\underset{\sim}{\theta}^T \underset{\sim}{z}(s))^2 \quad (2.14)$$

where

$$\underset{\sim}{z}(s) = \mathrm{col}[y(s+(k,\ell)),(k,\ell)\in N]$$

But $\ell n \det B(\underset{\sim}{\theta}) = \sum_{\Omega} \ell n(\mu_{ij})$ (2.15)

Substitution of (2.15) into (2.14) gives the desired log likelihood function. Due to the log likelihood function being non-quadratic in $\underset{\sim}{\theta}$, a gradient procedure such as Newton-Raphson may be used. Using "off the shelf" algorithms may be computationally expensive. We use the iterative scheme given below in (2.16) and (2.17) to estimate the parameters:

$$\bar{\underset{\sim}{\theta}}_{t+1} = [\underset{\sim}{R} - \frac{1}{\bar{\rho}_t}\bar{\underset{\sim}{S}}]^{-1}(\underset{\sim}{v} - \frac{1}{\bar{\rho}_t}\underset{\sim}{u}) \quad (2.16)$$

$$\bar{\rho}_t = \frac{1}{M^2}\sum_{s\in\Omega}(y(s)-\bar{\underset{\sim}{\theta}}_{t+1}\underset{\sim}{z}(s))^2 \quad (2.17)$$

$$\bar{\underset{\sim}{\theta}}_0 = \bar{\underset{\sim}{S}}^{-1}\underset{\sim}{u}, \quad \bar{\rho}_0 = \frac{1}{M^2}\sum_{s\in\Omega} (y(s)-\bar{\underset{\sim}{\theta}}_0^T \underset{\sim}{z}(s))^2$$

$$\underset{\sim}{v} = \sum_{(i,j)\in\Omega} \underset{\sim}{C}_{ij}, \quad \underset{\sim}{R} = \sum_{(i,j)\in\Omega} (\underset{\sim}{S}_{ij}\underset{\sim}{S}_{ij}^T - \underset{\sim}{C}_{ij}\underset{\sim}{C}_{ij}^T),$$

$$\underset{\sim}{C}_{ij}^T = \mathrm{col}[[\cos(\frac{2\pi}{M}((i-1)k+(j-1)\ell))], (k,\ell)\in N], \text{ M-vector}$$

$$\underset{\sim}{S}_{ij}^T = \mathrm{col}[\sin(\frac{2\pi}{M}((i-1)k+(j-1)\ell))], (k,\ell)\in N], \text{ M-vector}$$

$$\bar{\underset{\sim}{S}} = \sum_{s\in\Omega} z(s)\underset{\sim}{z}(s)^T, \quad \underset{\sim}{u} = \sum_{s\in\Omega} \underset{\sim}{z}(s)y(s)$$

Let $(\bar{\underset{\sim}{\theta}}, \bar{\rho})$ denote the final estimates of $(\underset{\sim}{\theta}, \rho)$. In the implementation of the restoration filters the estimates $\bar{\underset{\sim}{\theta}}$ and $\bar{\rho}$ obtained from Theorem 1 are used in the place of time parameters. For large values of M, the estimates $\bar{\underset{\sim}{\theta}}$ and $\bar{\rho}$ are close to the ML estimates and are asymptotically consistent and efficient. More discussion regarding the estimation scheme may be found in [15-16].

2.3 Error Analysis of the Restoration Algorithms

A desirable quantity to compute is the expected value of the minimum error . Since all our experiments were done for the case of degradation due to additive white noise, assume from now on that

$$\underset{\sim}{C} = \gamma \underset{\sim}{I} \,, \tag{2.18}$$

where γ is the noise variance. By substitution of (2.9) into (2.8), the following expression is obtained for the expected value of the minimum error e [1]:

$$e = \frac{1}{M^2} \operatorname{Tr}[\underset{\sim}{Q} - \underset{\sim}{L}\,\underset{\sim}{H}\,\underset{\sim}{Q}] \tag{2.19}$$

where

$$\underset{\sim}{L} = \underset{\sim}{Q}\,\underset{\sim}{H}^T(\underset{\sim}{H}\,\underset{\sim}{Q}\,\underset{\sim}{H}^T + C)^{-1}$$

Using the fact that the trace of a matrix is the sum of its eigenvalues,

$$e = \frac{1}{M^2} \operatorname{Tr}[\underset{\sim}{Q} - \underset{\sim}{L}\,\underset{\sim}{H}\,\underset{\sim}{Q}]$$

$$= \frac{1}{M^2} \sum_{\Omega} \frac{\rho}{||\mu_{ij}||^2} - \frac{\frac{\rho}{||\mu_{ij}||^2} h_{ij}^* \, h_{ij} \frac{\rho}{||\mu_{ij}||^2}}{\left(\frac{\rho}{||\mu_{ij}||^2} ||h_{ij}||^2 + \gamma\right)}$$

which after simplification gives

$$e = \frac{1}{M^2} \sum_{\Omega} \frac{\rho\gamma}{(\rho||h_{ij}||^2 + \gamma||\mu_{ij}||^2)} \tag{2.20}$$

3. Examples of Restoration

The algorithms described in Section 2 were implemented on different sizes of the standard USC "girl image" under different conditions.

Example 1 (Image with additive white Gaussian noise)

Figure 1(a) shows the original girl image of size 256x256 and intensity variations over the range 0-255. Since a 256x256 image may not be stationary, the image was divided into 16 blocks, each of size 64x64, and each block was modeled by a SAR model, with $N=\{(-1,0),(1,0),(0,-1),(0,1)\}$. Parameters were estimated using the iterative scheme in Section 2.2. Figure 1(b) shows the noisy image with SNR=7 db. The restoration algorithm in (2.13) was implemented and each block was restored independently. We emphasize that blocking was done due to considerations of stationarity alone and not due to any computational problems. The restored image is shown in Figure 1(c).

Due to the blocking, artificial lines are present in the restored image at known locations. These lines may be removed either in the Fourier transform domain or by a linear interpolation technique [2]. We used the latter technique. To remove vertical lines (3 pixels in width), each pixel in the lines was replaced by a linear weighted sum of neighboring pixels (including the current pixel) with weights 0.25, 0.2, 0.1, 0.2, 0.25. The image with vertical bars removed is in Figure 1(d). The same technique was used to remove the horizontal bars and the final restored picture is shown in Figure 1(e).

Example 2 (Image with blur and noise):

For this experiment, a 64x64 window of the original girl's face was used. The parameters corresponding to different neighbor sets were computed. The image was blurred by using the PSF

$$h(k,\ell) = \frac{0.4}{\pi} \exp\{-0.4(k^2+\ell^2)\} \tag{3.1}$$

and Gaussian noise of SNR=7 db was added. The results of implementing (2.12) are given in Figure 2 for different neighbor sets of dependence. Similar results for SNR=0 db are shown in Figure 3. The details of the neighbor sets used may be found in the figure caption.

To get some idea as to the amount of theoretical improvement that is possible, when using different neighbor sets, numerical values of the expected error e were computed using (2.20) for those neighbor sets. The quantity g defined as

$$g = 10 \log \frac{\text{MSE between original and degraded}}{e}$$

is tabulated in Table 1 for SNR=7 db and 0 db and for the blur function with PSF given in (3.1). The values of the numerator for SNR=7 db and 0 db were 511.41 and 1910.1 respectively. Although not reported here, the implementation for the case of colored noise can be done with equal ease.

Table 1

Performance bounds in decibels as predicted by various SAR models for the PSF in (3.1) and M=64.

Neighbor set N	SNR=7 db	SNR=0 db
{(-1,0),(0,-1),(-1,-1)} causal	4.687	8.678
{(-1,0),(1,0),(0,-1)}semi-causal	6.020	9.955
{(-1,0),(1,0),(0,-1),(0,1)} non-causal	5.634	8.641
{(-1,0),(0,1),(1,1),(1,0),(0,-1),(-1,-1)} non-causal	5.530	8.531
{(-1,0),(-1,1),(0,1),(1,0),(1,-1),(0,-1)} non-causal	4.630	6.811
{(-1,0),(-1,1),(0,1),(1,1),(1,0),(1,-1),(0,-1),(-1,-1)} non-causal	5.272	12.12

4. Discussion

We have developed restoration schemes using spatial autoregressive random field models. When dependence in all directions is included, the neighbors corresponding to the boundary pixels are not defined for these models. Hence some assumptions must be made regarding the distribution of these boundary pixels. It would be beneficial to make assumptions which aid in reducing excessive computations otherwise present in MMSE restoration problems, while at the same time not sacrificing any optimality properties. This leads to the problem of finding covariance matrices of SAR models that are diagonalized by fast transforms such as the FFT, sine or cosine transforms. By appropriately imposing some assumptions about the boundary pixels, covariance matrices which are diagonalized by these fast trasnforms can be realized [10]. We have used one such assumption, viz., that the images are represented on a toroidal lattice. The use of the torus lattice representation leads to the use of the FFT in the implementation of the filters, for any arbitrary neighbor set.

Such fast restoration filters have been considered in the literature [6-7] for different neighbor sets, using fast sine transforms. There are several disadvantages in using this formulation. Since the fast sine trasnforms diagonalize symmetric, tridiagonal Toeplitz matrices, the decomposition schemes suggested in [7] are valid only for isotropic neighbor sets. For instance, for the neighbor set $N = \{(0,-1),(1,0),(-1,0)\}$, it is required that $\theta_{1,0}=\theta_{-1,0}$. However, our experiments with this model and

the estimation scheme in Section 2 do not support this assumption. Also, when neighbor sets like $\{(-1,0),(1,0),(0,-1),(0,1),(1,1), (-1,-1),(-1,1),(1,-1),(0,2),(0,-2),(-2,0),(2,0)\}$ are considered, the resulting covariance matrices have banded Toeplitz structures and hence are not diagonalized exactly by sine transforms, so that approximate methods are required. On the other hand, the approach taken in this paper does not involve any such approximations. Given that some assumptions have to be made regarding the boundary pixels, it is preferable to make assumptions which have more general applicability.

The assumption of torus lattices can also be justified as follows: We computed the noramlized autocorrelation function at lower lags for different SAR models using the torus assumption and also by Fourier inversion of the spectral density function corresponding to some SAR models without the torus assumption. The numerical values differ in the second or third decimal place. Also, the torus assumption leads to an intuitively appealing relationship, viz., the eigenvalues of the covariance matrix are the two-dimensional discrete spectral density function.

We have also estimated the parameters of the underlying SAR models. The need for good estimates can be explained as follows. There is always a finite error in restoration; this error will be greater if the parameters characterizing the SAR models are not consistent or efficient. Though estimation schemes for unilateral neighbor sets are simple, they are not so for the SAR models considered here. By using the asymptotically consistent and

efficient estimates considered in this paper, the errors due to incorrect model specification can be reduced.

Fast Fourier transforms for image restoration using Wiener filters [1,17] have been considered earlier by approximating the block Toeplitz covariance structures by block circulant matrices. The important difference between the scheme developed here and the earlier schemes is in the characterization of signal statistics. The MMSE schemes need exact knowledge of the two-dimensional spectral density function (SDF). In practice it is not known. Hence, the true SDF is replaced by an estimate. Typical estimates of the SDF can be obtained by making suitable assumptions regarding the ACF as in [17], or by using estimates such as the FFTs of empirical covarance matrices. The former scheme assumes very simple functions for the ACF, while the latter uses inconsistent estimates of the SDF. In our approach, the true two-dimensional SDF is an explicit function of the parameters given by $S_y(\underset{\sim}{\theta},\rho,\nu_1,\nu_2) = \rho/||\mu_{ij}(\underset{\sim}{\theta})||^2$, where $\nu_1=\lambda_0 i, \nu_2=\lambda_0 j$. By using asymptotically consistent estimates like $S_y(\underset{\sim}{\overline{\theta}},\overline{\rho},\nu_1,\nu_2)$, as done here, better performance can be achieved. Also, the underlying structures of SAR models are more complicated and varied than that of the simple causal model in [17].

References

1. H. C. Andrews and B. R. Hunt, Digital Image Restoration, Prentice-Hall, Inc., NJ, 1977.

2. A. Rosenfeld and A. C. Kak, Digital Picture Processing, Academic Press, NY, 1976.

3. D. P. Panda and A. C. Kak, "Recursive Least Squares Smoothing of Noise in Images," IEEE Trans. on Acoustics, Speech and Signal Processing, Vol. ASSP-25, pp. 520-524, Dec. 1977.

4. M. S. Murphy and L. M. Silverman, "Image Model Representation and Line by Line Recursive Restoration, IEEE Trans. on Automatic Control, Vol. AC-23, pp. 808-816, Oct. 1978.

5. J. W. Woods and C. H. Radewan, "Kalman Filtering in Two Dimensions," IEEE Trans. on Information Theory, Vol. IT-23, pp. 473-482, July 1977.

6. A. K. Jain, "An Operator Factorization Method for Restoration of Blurred Images," IEEE Trans. on Computers, Vol. C-26, pp. 1061-1072, Nov. 1977.

7. A. K. Jain and J. R. Jain, "Partial Difference Equations and Finite Differences in Image Processing--Part II: Image Restoration," IEEE Trans. on Automatic Control, Vol. AC-23, pp. 817-833, Oct. 1978.

8. P. Whittle, "On Stationary Processes in the Plane," Biometrika, Vol. 41, pp. 434-449, 1954.

9. R. L. Kashyap, "Univariate and Multivariate Random Field Models for Images," Computer Graphics and Image Processing, Vol. 12, pp. 257-270, March 1980.

10. R. L. Kashyap, "Random Field Models on Torus Lattices for Finite Images," Proc. 5th Int. Conf. on Pattern Recognition, Miami, Florida, Dec. 1980.

11. M. Hassner and J. Sklansky, "The Use of Markov Random Fields as Models of Textures," Computer Graphics and Image Processing, Vol. 12, pp. 357-370, April 1980.

12. J. Besag, "Spatial Interaction and Statistical Analysis of Lattice Systems," Jl. Royal Stat. Soc., Ser. B., Vol. B-36, pp. 199-236, 1974.

13. J. W. Woods, "Two-dimensional Discrete Markov Random Fields," IEEE Trans. on Information Theory, Vol. 18, pp. 232-240, March 1972.

14. R. L. Kashyap and R. Chellappa, "Image Restoration Using Random Field Models," Proc. of the 18th Annual Allerton Conf. on Commn., Control and Computing, Univ. of Illinois, Urbana, Ill., Oct. 1980.

15. R. Chellappa, "Fitting Random Field Models to Images," Tech. Report TR-928, Computer Science Center, University of Maryland, College Park, Md., 20742, Aug. 1980.

16. R. Chellappa and R. L. Kashyap, "Synthetic Generation and Estimation in Random Field Models of Images" (submitted for publication).

17. W. K. Pratt and F. Davarian, "Fast Computational Techniques for Pseudo Inverse and Wiener Image Restoration," IEEE Trans. on Computers, Vol. C-26, pp. 571-580, June 1977.

(a)

(b)

(c)

(d)

(e)

Fig.1. Restoration of a noisy image:

a) original

b) noisy SNR = 7 db

c) restored image (note the presence of lines due to blocking)

d) vertical lines removed

e) final restored image.

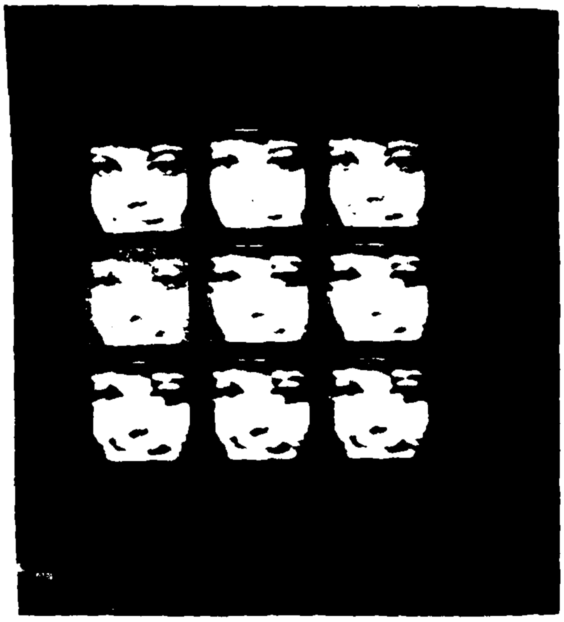

Fig. 2. Restoration of image containing blur (4.1) and Gaussian noise
(1,1): Original;
(1,2): Blurred image;
(1,3): Restored image, SNR = α;
(2,1): Blur and noise (7 db);
(2,2): Restoration with N = {(0,-1),(-1,0),(-1,-1)};
(2,3): N = {(-1,0)(1,0),(0,-1)};
(3,1): N = {(0,1),(0,-1),(-1,0),(1,0)};
(3,2): N = {(0,1),(1,0),(0,-1),(-1,0),(0,-1),(-1,0)};
(3,3): N = {(0,1),(0,-1),(1,0),(1,1),(-1,-1),(-1,1),(1,-1)}.

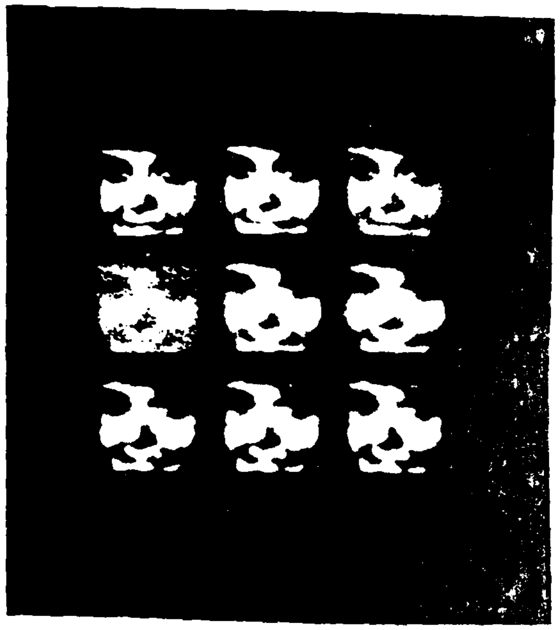

Fig. 3. Similar to Fig. 2 with SNR = 0 db.

DATE
FILMED

-8